Heliyon 10 (2024) e33525

Contents lists available at ScienceDirect

Heliyon

journal homepage: www.cell.com/heliyon

Research article

Telomere length as a predictor of therapy response and survival in patients diagnosed with ovarian carcinoma

Kristyna Tomasova [a,b,1,*], Karolina Seborova [c,d,1], Michal Kroupa [a,b], Josef Horak [a,e], Miriam Kavec [a,f], Ludmila Vodickova [a,b,g], Lukas Rob [h], Martin Hruda [h], Marcela Mrhalova [i], Alena Bartakova [j], Jiri Bouda [j], Thomas Fleischer [k], Vessela N. Kristensen [l], Pavel Vodicka [a,b,g,2], Radka Vaclavikova [c,d,2]

[a] Department of Molecular Biology of Cancer, Institute of Experimental Medicine of the Czech Academy of Sciences, Videnska 1083, 142 00, Prague, Czech Republic
[b] Biomedical Center, Faculty of Medicine in Pilsen, Charles University, Alej Svobody 1655/77, 32300, Pilsen, Czech Republic
[c] Toxicogenomics Unit, National Institute of Public Health, Srobarova 48, 100 42, Prague, Czech Republic
[d] Laboratory of Pharmacogenomics, Biomedical Center, Faculty of Medicine in Pilsen, Charles University, Alej Svobody 1655/76, 323 00, Pilsen, Czech Republic
[e] Third Faculty of Medicine, Charles University, Ruska 87, 100 00, Prague, Czech Republic
[f] Department of Oncology, First Faculty of Medicine, Charles University and Thomayer Hospital, Prague, Czech Republic
[g] Institute of Biology and Medical Genetics, First Faculty of Medicine, Charles University, Albertov 4, 128 00, Prague, Czech Republic
[h] Department of Gynecology and Obstetrics, Third Faculty of Medicine, Charles University and University Hospital Kralovske Vinohrady, Prague, Czech Republic
[i] Department of Pathology and Molecular Medicine, Second Faculty of Medicine and Motol University Hospital, Charles University, Prague, Czech Republic
[j] Department of Gynecology and Obstetrics, Faculty of Medicine and University Hospital in Pilsen, Charles University, Pilsen, Czech Republic
[k] Department of Cancer Genetics, Institute for Cancer Research, Oslo University Hospital, The Norwegian Radium Hospital, Oslo, Norway
[l] Department of Medical Genetics, Institute of Clinical Medicine, Faculty of Medicine, University of Oslo, Oslo, Norway

ARTICLE INFO

Keywords:
Telomere length
Ovarian cancer
Shelterin
Telomerase
Therapy response

ABSTRACT

Impaired telomere length (TL) maintenance in ovarian tissue may play a pivotal role in the onset of epithelial ovarian cancer (OvC). TL in either target or surrogate tissue (blood) is currently being investigated for use as a predictor in anti-OvC therapy or as a biomarker of the disease progression, respectively. There is currently an urgent need for an appropriate approach to chemotherapy response prediction.

We performed a monochrome multiplex qPCR measurement of TL in peripheral blood leukocytes (PBL) and tumor tissues of 209 OvC patients. The methylation status and gene expression of

* Corresponding author. Department of Molecular Biology of Cancer, Institute of Experimental Medicine, Czech Academy of Sciences, Videnska 1083, 142 00, Prague, Czech Republic.

E-mail addresses: kristyna.tomasova@iem.cas.cz (K. Tomasova), karolina.seborova@szu.cz (K. Seborova), michal.kroupa@iem.cas.cz (M. Kroupa), josef.horak@iem.cas.cz (J. Horak), miriam.kavec@gmail.com (M. Kavec), ludmila.vodickova@iem.cas.cz (L. Vodickova), lukas.rob@lf3.cuni.cz (L. Rob), martin.hruda@lf3.cuni.cz (M. Hruda), marcela.mrhalova@lfmotol.cuni.cz (M. Mrhalova), bartakovaa@fnplzen.cz (A. Bartakova), boudaj@fnplzen.cz (J. Bouda), thomas.fleischer@rr-research.no (T. Fleischer), v.n.kristensen@medisin.uio.no (V.N. Kristensen), pavel.vodicka@iem.cas.cz (P. Vodicka), radka.vaclavikova@szu.cz (R. Vaclavikova).

[1] These authors contributed equally to this work.
[2] Shared senior authorship.

https://doi.org/10.1016/j.heliyon.2024.e33525
Received 18 July 2023; Received in revised form 14 June 2024; Accepted 23 June 2024
Available online 29 June 2024

the shelterin complex and telomerase catalytic subunit (*hTERT*) were determined within tumor tissues by High-Throughput DNA methylation profiling and RNA sequencing (RNA-Seq) analysis, respectively. The patients sensitive to cancer treatment (n = 46) had shorter telomeres in PBL compared to treatment-resistant patients (n = 93; P = 0.037). In the patients with a different therapy response, transcriptomic analysis showed alterations in the peroxisome proliferator-activated receptor (PPAR) signaling pathway (q = 0.001). Moreover, tumor TL shorter than the median corresponded to better overall survival (OS) (P = 0.006). *TPP1* gene expression was positively associated with TL in tumor tissue (P = 0.026).

TL measured in PBL could serve as a marker of platinum therapy response in OvC patients. Additionally, TL determined in tumor tissue provides information on OvC patients' OS.

Abbreviations

ADIPOQ	adiponectin
AMPK	adenosine monophosphate-activated protein kinase
ATM kinase	ataxia-telangiectasia mutated kinase
ATR kinase	ataxia-telangiectasia and Rad3-related kinase
AUC	area under the curve
BCL7A	B-cell CLL/lymphoma 7 A
BH	Benjamini and Hochberg
bp	base pairs
BRCA1	breast cancer 1
BRCA2	breast cancer 2
c-MYC	c-MYC proto-oncogene
CASC1	cancer susceptibility candidate gene 1
CD36	cluster determinant 36
CFAP45	cilia and flagella associated protein 45
CLDN11	claudin 11
CLDN18	claudin 18
CLPTM1L	cleft lip and palate transmembrane protein 1-like protein
CpG	cytosine-phosphate-guanine
DE	differential expression
DKC1	dyskerin pseudouridine synthase 1
dsDNA	double-stranded DNA
EFHC2	EF-hand domain containing 2
FABP4	fatty acid binding protein 4
FIGO	International Federation of Gynecology and Obstetrics
FMR1	fragile X messenger ribonucleoprotein 1
GO	gene ontology
GSEA	Gene set enrichment analysis
GWAS	genome-wide association studies
HNF4A	hepatocyte nuclear factor 4 alpha
HNRNPAB	heterogenous nuclear ribonucleoprotein A/B
hTERC	telomerase RNA component
hTERT	telomerase reverse transcriptase
HYDIN	axonemal central pair apparatus protein
JAM3	junction adhesion molecule 3
KDM2A	lysine demethylase 2 A
KEGG	Kyoto Encyclopedia of Genes and Genomes
KLB	klotho beta
$\log_2$ FC	$\log_2$ fold change
LPL	lipoprotein lipase
NASP	nuclear autoantigenic sperm protein
NR4A3	nuclear receptor 4A3
OS	overall survival
OvC	ovarian cancer
PBL	peripheral blood leukocytes
PCA	principal component analysis
PFI	platinum-free interval
PIGR	polymeric immunoglobulin receptor
PLIN2	perilipin 2
POLE3	DNA polymerase epsilon 3
POT1	protection of telomeres 1
PPAR	peroxisome proliferator-activated receptor
qPCR	quantitative polymerase chain reaction

1. Introduction

Human telomeres are made of highly conserved tandem nucleic acid repeats and associated proteins of the shelterin complex located at the ends of chromosomes [1]. The shelterin subunits, namely telomere protective protein 1 (TPP1), repressor/activator protein 1 (RAP1), telomeric repeat binding factor 1 (TERF1) and 2 (TERF2), TERF1-interacting nuclear factor 2 (TIN2), and protection of telomeres 1 (POT1), together with DNA repair, maintain the protective function of telomeres [2]. The chromosome end-cap structure consists of telomeric single-stranded DNA (ssDNA) invading telomeric double-stranded DNA (dsDNA) sites to hide the 3'-terminus [3]. The assembly of shelterin at telomeres encompasses the binding of POT1-TPP1 to ssDNA overhang, TERF1 and TERF1-RAP1 to dsDNA, and TIN2 to the whole complex by simultaneous interaction with TERF1, TERF2, and TPP1, which keeps the telomeres intact [4]. Shelterin prevents telomere hyper-resection by suppressing DNA damage response kinases [5]. While TERF2 binds and inhibits ataxia-telangiectasia mutated (ATM) kinase, the POT1-TPP1 heterodimer blocks ataxia-telangiectasia and Rad3-related (ATR) kinase activation [5]. Deregulation of telomere maintenance can give rise to cancer [6]. Cancerous cells, unlike almost all somatic cells under physiological conditions, can fix eroded telomeres via either telomerase reactivation or by a homologous recombination-based pathway known as alternative lengthening of telomeres [7]. The majority of cancers, however, rely on telomerase reactivation [8]. Telomerase is a ribonucleoprotein polymerase composed primarily of the telomerase reverse transcriptase (hTERT) and telomerase RNA component (hTERC), together with other associated proteins [9].

Ovarian cancer (OvC), a heterogeneous group of diseases characterized by distinct clinicopathological and molecular patterns, may be driven by telomere dysfunction [10,11]. According to current knowledge, ovarian tumors appear to be strictly telomerase-dependent [10]. Substantial *hTERT* expression, a limiting factor for telomerase catalytical activity, exhibits 95 % of ovarian tumors [10]. The harboring of *hTERT* promoter mutation was reported in 16 % of clear cell OvC [12,13] and 50 % of granulosa cell tumors [14].

Currently, not much is known about shelterin impairment in OvC tissue. *POT1* knockdown in OvC-derived SK-OV3 cells reduces c-MYC proto-oncogene (*c-MYC*) expression, causing temporary inhibition of proliferation, but ultimately results in enhanced cell division, tumorigenicity, and histone deacetylase inhibitor response [15]. c-MYC protein mediates the regulation of telomerase activity, and changes in its transcription upset the balance of the telomere/telomerase system [16]. Among the 22 genes related to telomere structure, length, and maintenance, genome-wide association studies (GWAS) identified single nucleotide polymorphisms (SNPs) rs116895242 in the *POT1,* rs7717443, rs10866498, rs12655062, rs2736098 in the *hTERT*, and rs75316749 in the *hTERC-CLPTM1L* (cleft lip and palate transmembrane protein 1-like protein) regions, to be associated with OvC risk [17].

In this study, we investigated tumor and peripheral blood leukocyte (PBL) telomere length (TL) of patients diagnosed with late-stage OvC, along with *hTERT* and shelterin genes' methylation/mRNA expression in the tumor tissue. We were also interested in the possible connection between TL assessed in PBL/tumor tissue and therapy response. In this article, we hypothesize that patients' response to treatment and survival may be predicted by the TL either in PBL, representing a surrogate tissue of the patients or in the tumor tissue itself. We further hypothesize that the mRNA expression and DNA methylation of shelterin subunits and telomerase may be mirrored by TL.

2. Materials and methods

2.1. Study population

Overall, the study comprised 212 OvC patients, of which 184 were sampled for peripheral blood at the time of diagnosis and 59 for tumor tissue during surgical resection. Thirty-one patients were sampled for both tumor tissue and peripheral blood. Regarding the tumor tissue, data from RNA sequencing (RNA-Seq) were available for all the patients, data from the methylation arrays were available only from 58 patients, and telomeres were successfully measured within 56 patients. As for blood, TL was assessed in all 184 samples. The patients were women with newly diagnosed and histologically confirmed OvC. All patients were diagnosed and treated between

S	single-copy gene
SMC1A	structural maintenance of chromosomes 1 A
SNP	single nucleotide polymorphism
ssDNA	single-stranded DNA
SSRP1	structure specific recognition protein 1
T	telomere
TERF1	telomeric repeat binding factor 1
TERF2	telomeric repeat binding factor 2
TIN2	TERF1-interacting nuclear factor 2
TL	telomere length
TPP1	telomere protective protein 1
TSS	transcription start site
UPF1	DNA helicase and adenosine triphosphatase
UTR	untranslated region
YEATS4	YEATS domain containing 4

2009 and 2019 at the Motol University Hospital in Prague, and the University Hospital in Pilsen, Czech Republic. Biological samples for genetic analyses were obtained from all patients according to the Helsinki declaration. Table 1 summarizes the characteristics of all 212 patients, Table 2 only of 31 patients with both tumor and blood collected. Sensitivity to the OvC therapy was based on the platinum-free interval (PFI) described by Friedlander et al. [18], separating OvC patients as having platinum-sensitive or platinum-resistant disease. The PFI interval was defined as the time from the last dose of platinum-based chemotherapy to the progression of the disease. Patients with PFI≤6 months were considered platinum-resistant (this group also included OvC patients with intermediate PFI – 6 to 12 months), and patients with PFI≥12 months were platinum-sensitive. Overall survival (OS) of the investigated OvC patients was based on the interval from the surgery to the date of death or last follow-up. The follow-up was conducted over 10 years.

2.2. DNA sample isolation and quantification

Tumor DNA was isolated from fresh frozen tumor tissue after pulverization in liquid nitrogen using AllPrep DNA/RNA/Protein Mini Kit (Qiagen, Hildesheim, Germany). Genomic DNA from 250 μL of peripheral blood was performed by BioSprint DNA Blood Kit (Qiagen, Valencia, CA, USA) using Kingfisher mL instrument (ThermoFisher Scientific, Waltham, MA, USA) according to manufacturer protocol. Isolated DNA was quantified by Quant-iT PicoGreen dsDNA Reagent and Kits (ThermoFisher Scientific, Waltham, MA, USA)

Table 1
All patients' characteristics. The table shows the characteristics of all patients participating in the study. The number of patients does not always add up to 100 % (n = 212) due to missing data for some attributes.

A studied cohort of patients	Median age (years) [range]	60.92 [24–89]	%
		n = 212	
Tumor type			
	low-grade serous	9	4.2
	high-grade serous	162	76.4
	mucinous	11	5.2
	clear cell	9	4.2
	endometrioid	4	1.9
	Brenner	1	0.5
	borderline	1	0.5
	adenocarcinoma	4	1.9
	generalized disease	1	0.5
Grade			
	1	7	3.3
	2	19	9.0
	3	165	77.8
FIGO stage[a]			
	I	9	4.2
	II	12	5.7
	III	156	73.6
	IV	15	7.1
Residual tumor[b]			
	yes	102	48.1
	no	90	42.5
***BRCA1/BRCA2* mutation**[c]			
	yes	13	6.1
	no	199	93.9
Therapy regimen			
	paclitaxel + platinum derivatives	162	76.4
	platinum monotherapy	6	2.8
	other regimen[d]	10	4.7
	none	1	0.5
Platinum-based therapy resistance			
	yes	60	28.3
	no	106	50.0
Median p**latinum-free interval (PFI, months) [range]**			
	platinum-resistant	5.31 (0–11.5)	
	platinum-sensitive	29.06 (12–97)	

[a] FIGO (International Federation of Gynecology and Obstetrics) staging system is used for ovarian, fallopian tube, and peritoneal cancer classification.

[b] Residual tumor after surgery was defined by a surgeon as "yes" (macroscopic lesions <1 cm and peritoneal metastases >1 cm), or "no" [no macroscopic residuum (R)].

[c] Breast cancer 1 and 2 (*BRCA1/2*) germline mutations are the most frequent causes of developing hereditary OvC.

[d] Other regimen [paclitaxel + platinum derivate + cyclofosfamid, cisplatin + doxorubicin, oxaliplatin + capecitabine (known as XELOX), oxaliplatin + 5-fluorouracil + folinic acid (known as FOLFOX) administered in a regimen called modified FOLFOX6, or paclitaxel + carboplatin + bevacizumab].

Table 2
Characteristics of patients with both blood and tumor tissue samples. The table shows the characteristics of all patients from whom we could analyze both tissue and blood. The number of patients does not always add up to 100 % (n = 31) due to missing data for some attributes.

A studied cohort of patients	Median age (years) [range]	58.77 [40–77]	%
		n = 31	
Tumor type			
	low-grade serous	3	9.7
	high-grade serous	21	67.7
	mucinous	3	9.7
	clear cell	3	9.7
	endometrioid	0	0.0
	Brenner	0	0.0
	borderline	0	0.0
	adenocarcinoma	0	0.0
	generalized disease	0	0.0
Grade			
	1	2	6.5
	2	3	9.7
	3	26	83.9
FIGO stage[a]			
	I	2	6.5
	II	1	3.2
	III	25	80.6
	IV	2	6.5
Residual tumor[b]			
	yes	18	58.1
	no	13	41.9
***BRCA1/BRCA2* mutation**[c]			
	yes	5	16.1
	no	26	83.9
Therapy regimen			
	paclitaxel + platinum derivatives	31	100
	platinum monotherapy	0	0
	other regimen[d]	0	0
	none	0	0
Platinum-based therapy resistance			
	yes	10	32.3
	no	21	67.7
Median platinum-free interval (PFI, months) [range]			
	platinum-resistant	4.35 (0.5–8)	
	platinum-sensitive	38.47 (15–97)	

[a] FIGO staging system is used for ovarian, fallopian tube, and peritoneal cancer classification.
[b] Residual tumor after surgery was defined by a surgeon as "yes" (macroscopic lesions <1 cm and peritoneal metastases >1 cm), or "no" (no macroscopic residuum).
[c] *BRCA1/2* germline mutations are the most frequent causes of developing hereditary OvC.
[d] Other regimen [paclitaxel + platinum derivate + cyclofosfamid, cisplatin + doxorubicin, oxaliplatin + capecitabine (known as XELOX), oxaliplatin + 5-fluorouracil + folinic acid (known as FOLFOX) administered in a regimen called modified FOLFOX6, or paclitaxel + carboplatin + bevacizumab].

and the plate reader Infinite 200 (Tecan Group Ltd., Männedorf, Switzerland).

2.3. Telomere length measurement

TL in PBL and tumor tissues was expressed as relative by the monochrome multiplex quantitative polymerase chain reaction (qPCR) method, as described in detail previously [19,20]. Briefly, Ct values for telomere sequences (T) and reference single-copy gene (S; albumin) were determined simultaneously as a multiplex using ViiA 7 Real-time PCR System (Applied Biosystems, Foster City, CA, USA). The standard curve was used to quantify telomere and albumin genes based on the respective cycle threshold values. TL was expressed as the ratio between the T/S. PBL TL was measured using DNA from the whole blood since erythrocytes do not have a nucleus containing telomeric sequences. The qPCR efficiency for telomere sequences in tissues was 93 % and 91 % for albumin. The reaction efficiency for telomere sequences in blood ranged between 98–110 % and 90–104 % for the albumin gene. All the data were normalized based on the qPCR efficiency, as described previously [21].

2.4. RNA sequencing library preparation and sequencing

The total RNA from 59 epithelial OvC tissues with an RNA integrity number (RIN) > 5.4 (mean RIN 8.5, range 5.4–9.9) was used for RNA-Seq analysis (summarized in detail in Supplementary Table 1). Five hundred ng of the total RNA was used for library preparation

with QuantSeq 3′mRNA-Seq Library Prep FWD for Illumina (Lexogen, Vienna, Austria) according to the manufacturer's protocol. The quality of the prepared libraries was checked by Bioanalyzer 2100 using the High Sensitivity DNA kit (Agilent Technologies Inc., Santa Clara, CA, USA), and the quantity was measured by qPCR, KAPA Library Quantification Kit Illumina®Platforms (F.Hoffmann-La Roche AG, Basel, Switzerland). The equimolar pool of prepared libraries was sequenced on the NextSeq 500 platform (Illumina Inc., San Diego, CA, USA) using the NextSeq 500 High Output v2 Kit (75 cycles) in one run, with a 1 × 75 base pairs (bp) setting, aimed at 6–7 million reads per sample.

2.4.1. mRNA expression analysis

Raw RNA-Seq data quality was checked by FastQC [22] v0.12.0 and MultiQC [23] v1.14 tools and the fastp v0.23.3 package, which was also used for quality filtering and adapter trimming [24]. Gene annotation was based on reference transcriptome GENCODE v35 (GRCh38.p13). Protein-coding gene abundance was estimated by kallisto tool v0.50.1 using a pseudoalignment approach [25].

For all RNA-Seq analyses of mRNA transcripts, we used R v4.4.0 (R Core Team). Genes with zero counts or one count across the samples were removed before analysis, resulting in 18,462 protein-coding genes out of 19,972 for further analysis. Differential expression analysis of mRNAs was carried out by the DESeq2 package v1.44.0 with default settings [26]. The false discovery rate was managed by the Benjamini and Hochberg (BH) method for P values and by ashr for $\log_2$ fold change ($\log_2$ FC) values [27], both in the DESeq2 package. Statistically differentially expressed genes were considered genes with $q < 0.05$ (P value after BH correction).

Gene set enrichment analysis (GSEA) was performed by clusterProfiler v4.12.0 and DOSE v3.30.1 packages in R v4.4.0 [28, 29]. Gene ontology (GO) and Kyoto Encyclopedia of Genes and Genomes (KEGG) databases were used to explore the biological function of differentially expressed genes [30–32]. As statistically significant enrichment we counted the results with Bonferonni corrected $q < 0.05$.

2.5. High-Throughput DNA methylation profiling

The genome-wide DNA methylation profile was analyzed by Infinium MethylationEPIC BeadChip microarrays (Illumina Inc.) in 58 epithelial OvC tissues. Five hundred ng of DNA was used as input for bisulfite conversion according to the manufacturer's manual by EZ DNA Methylation™ Kit (Zymo Research, Irvine, CA, USA). Prepared microarrays were scanned by iSCAN System (Illumina Inc.).

2.5.1. Methylation analysis

Quality control and data normalization were performed by the SWAN approach by the minfi package in the R v4.4.0 (R Core Team) as described previously [33–35]. Raw data were converted to β values for further analyses [36–38]. Probes with annotated SNP were removed before analyses [39]. For analysis of gene regions, the probes were then collapsed into specific gene regions based on the manifest for the microarray – TSS200 [cytosine-phosphate-guanine (CpG) between TSS (transcription start site) and 200bp upstream

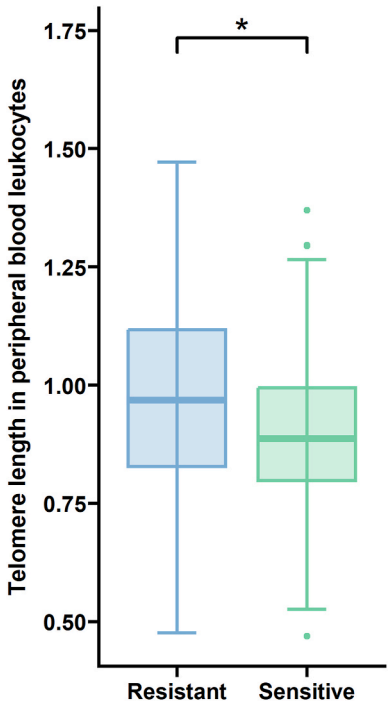

Fig. 1. Shorter PBL TL may be coupled with enhanced sensitivity to OvC therapy. Patients responding to treatment (>12 months, n = 93) have shorter telomeres than those therapy-resistant (1–6 months, n = 46, **P = 0.037**).

and TSS itself], TSS1500 (CpG between TSS and 1500–200bp upstream), 5′UTR [CpG in 5′ untranslated region (UTR)], 1stExon (CpG in the first exon), gene body (CpG in other exons or introns), 3′UTR (CpG in 3′UTR region) as described previously [40]. The promoter region defined a combination of CpG in TSS200 and TSS1500. We focused on the whole gene, TSS200, TSS1500, and promoter methylation profiles. The degree of gene methylation was divided according to Bibikova et al. [41]: 0.00–0.29 (unmethylated/hypomethylated), 0.30–0.79 (hemimethylated), and 0.80–1.00 (methylated/hypermethylated). For the correlation with expression, we used β values from the promoter probes (TSS1500 and TSS200 together).

2.6. Statistical analysis

Statistical analyses and graphs were made in the R v4.4.0 (R Core Team) environment. The Dplyr package was used for the data

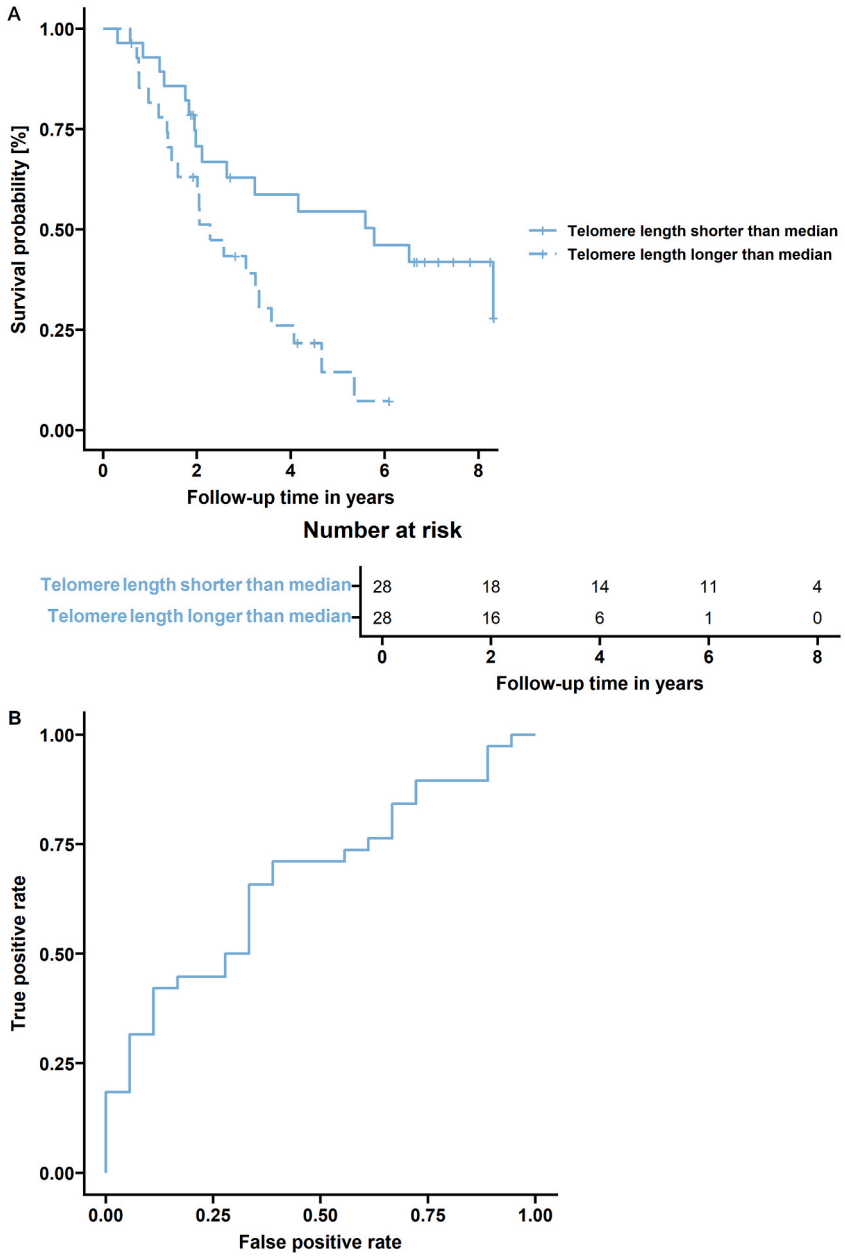

Fig. 2. OS of patients could be predicted by TL in tumor tissue. A) The group with tumor TL higher than the median had poorer OS (n = 56, **P = 0.006**). The table illustrates how many patients were at risk in two-year intervals. **B)** The 56 patients were divided according to their follow-up to those who died (n = 38) and those who were at the time of their last control still alive (n = 18). As a marker, the tumor TL was selected. The area under the curve (AUC) = 0.673 confirmed that the tumor TL might be indicative of OvC patients' OS.

manipulation, survival, and survminer packages for the calculation of survivals, and the ggplot2 package for the plot rendering. For the evaluation of the normal distribution, we used the Shapiro-Wilk test. In the case of normal distribution, parametric tests were used (*t*-test, ANOVA), and in the case of non-normal distribution, non-parametric tests were used (Mann-Whitney and Kruskal-Wallis tests). For survival, the log-rank test was used. For all tests, a $P < 0.05$ was considered significant.

3. Results

3.1. Telomere length in peripheral blood leukocytes predicts response to therapy

TL was measured within 184 patients with the availability of PBL samples. However, 22 patients were excluded from the analysis since information about chemotherapy administration was not available. Therefore, the total number of patients with information about blood sampling before chemotherapy (n = 136) and after chemotherapy treatment (n = 26) was 162. TL measured in PBL within the groups of patients sampled before (n = 136) and after chemotherapy (n = 26) did not significantly differ (parametrical *t*-test, P = 0.15). Importantly, therapy-sensitive individuals (n = 93) were associated with shorter telomeres in PBL compared to PBL in the patients with treatment resistance (n = 46, parametrical *t*-test, **P = 0.037**), as seen in Fig. 1. Thirty-nine patients did not have a record of the treatment response, and they were not included in the analysis. Patients with postoperative tumor residues (n = 89) did not differ in their PBL TL from those with tumors completely removed (n = 78, parametrical *t*-test, P = 0.181). Seventeen patients from 184 had the information about tumor residuum missing. Macroscopic residuum is estimated by the surgeon by the end of the debulking surgery using a combination of visual inspection and palpable examination, and it is characterized into three groups: R0 (no macroscopic residuum), R1 (macroscopic residuum <1 cm), and R2 [macroscopic residuum (metastases) >1 cm].

3.2. Telomere length in tumor tissue reflects the survival of ovarian cancer patients

TL exceeding the median [0.75 (0.74–1.94)] in tumor tissue was independently associated with OS in our studied group of patients (log-rank test, n = 56, **P = 0.006**), as illustrated in Fig. 2. However, neither OS (log-rank test, P = 0.39) nor the time to progression (log-rank test, P = 0.18) was associated with PBL TL in our patients (n = 184).

3.3. Association of telomere length in peripheral blood leukocytes and tumor tissue with other clinicopathological characteristics of the patients

No TL differences in either PBL or tumor tissue of the patients diagnosed with different tumor histotypes were observed [high-grade serous carcinoma (n = 145 for PBL, n = 37 for tissue), low-grade serous carcinoma (n = 8 for PBL, n = 4 for tissue), mucinous carcinoma (n = 6 for PBL, n = 8 for tissue), and clear cell carcinoma subtype (n = 7 for PBL, n = 4 for tissue), ANOVA, P = 0.68, and P = 0.94, respectively]. Furthermore, patients diagnosed with high-grade serous carcinoma (n = 145 for PBL, n = 37 for tissue), the most malignant form of the disease, did not have significantly different TL in either PBL or tumor compared to the patients with other subtypes of the tumors with epithelial origin (n = 21 for PBL, n = 16 for tissue, Mann-Whitney *U* test, P = 0.95, P = 0.11, respectively).

The stage of the disease based on the FIGO system was not associated with TL differences in either PBL or tumor tissue in our studied group of patients [FIGO stage I + II (n = 17 for PBL, n = 7 for tissue), FIGO stage III + IV (n = 148 for PBL, n = 48 for tissue), Mann-

Table 3
PBL and tumor TL in patient subgroups. The table summarizes TL data measured in PBL and tumor tissues of patients diagnosed with OvC, along with various personal and clinicopathological characteristics.

	PBL				Tumor tissue			
	n = 184	**%**	**Median TL (range)**	**P-value**	**n = 56**	**%**	**Median TL (range)**	**P-value**
				Tumor type				
low-grade serous	8	5	0.81 (0.71–1.25)	0.68 (ANOVA)	4	7.5	0.77 (0.69–0.99)	0.94 (ANOVA)
high-grade serous	145	87	0.91 (0.45–1.47)		37	70	0.68 (0.13–2.11)	
mucinous	6	4	0.91 (0.76–1.47)		8	15	0.77 (0.33–1.47)	
clear cell	7	4	0.94 (0.80–1.29)		4	7.5	0.95 (0.23–1.36)	
				Grade				
1	5	3	0.82 (0.76–1.47)	0.60 (ANOVA)	4	7	0.72 (0.69–0.99)	1 (ANOVA)
2	14	9	0.91 (0.63–1.23)		8	14	0.87 (0.28–1.47)	
3	145	88	0.91 (0.46–1.47)		44	79	0.75 (0.13–2.11)	
				FIGO stage				
I + II	17	10	0.85 (0.63–1.47)	0.44 (Mann-Whitney)	7	13	0.69 (0.28–1.54)	0.91 (Mann-Whitney)
III + IV	148	90	0.92 (0.46–1.47)		48	87	0.79 (0.13–2.11)	
				Residual tumor				
yes	89	53	0.90 (0.47–1.40)	0.18 (*t*-test)	31	55	0.81 (0.17–1.47)	0.74 (*t*-test)
no	78	47	0.92 (0.46–1.47)		25	45	0.69 (0.13–2.11)	
				Therapy resistance				
yes	46	33	0.97 (0.48–1.47)	**0.037** (*t*-test)	23	41	0.81 (0.17–1.54)	0.45 (*t*-test)
no	93	67	0.89 (0.47–1.37)		33	59	0.72 (0.13–2.11)	

Whitney *U* test, P = 0.44, and P = 0.91, respectively]. The grade of the disease was not associated with TL differences in either PBL or tumor tissue [grade 1 (n = 5 for PBL, n = 4 for tissue), grade 2 (n = 14 for PBL, n = 8 for tissue), grade 2 (n = 145 for PBL, n = 44 for tissue), ANOVA, P = 0.60, P = 1, respectively]. Also, TL in PBL [median (range), 0.91 (0.47–1.29)] did not correlate with TL measured in tumor tissue [median (range), 0.75 (0.74–1.94), n = 31, Pearson correlation coefficient, R = −0,168, P = 0.99].

All TL values measured in PBL or OvC tissue and the results, presented in **3.1**–**3.3,** are displayed in Table 3. The TL data were not age-adjusted due to the lack of relationship between TL in either PBL (n = 184) or tumor tissue (n = 56) and age at the time of diagnosis or clinical surgery (Kendall rank correlation coefficient, R = −0.045, P = 0.37; R = 0.11, P = 0.36 respectively).

3.4. Methylation status of shelterin subunits and hTERT correlates with telomere length in tumors

DNA hypermethylation within the *TERF1* body and hypomethylation of the promoter sequence TSS1500 positively correlated with TL (n = 58, Kendall rank correlation coefficient, **P = 0.0001**, **P = 0.0007**, respectively). The *TPP1* gene body hosting CpG hypomethylation was positively associated with TL **(**n = 58, Kendall rank correlation coefficient, **P = 0.003)**. *RAP1* 3′UTR hypermethylation and TL inversely correlated (n = 58, Kendall rank correlation coefficient, **P = 0.002).** DNA hemimethylated status in *hTERT* transcriptional start site TSS1500 and *TERF2* gene body negatively correlated with TL (n = 58, Kendall rank correlation coefficient, **P = 0.0003** and **P = 0.0001** for *hTERT*; and **P = 0.0009** for *TERF2*). Additionally, methylation of *hTERT* promoter TSS1500 negatively correlated with the gene mRNA expression levels (n = 58, Kendall rank correlation coefficient, R = −0.21, **P = 0.025**, see Fig. 3). However, the methylation status of none of the shelterin complex genes investigated in the study (*TERF1*, *TERF2*, *TPP1*, *RAP1*, *POT1*, and *TIN2*) was associated with the expression levels of the genes (P values not shown).

After the correction for all genes tested, the positive association between *TERF1* hemimethylated status and TL remained significant (n = 58, Kendall rank correlation coefficient, **P = 0.005**). Following the correction for all tested probes, hemimethylated *hTERT* TSS1500 negatively and hypermethylated *TERF1* body positively correlated with TL (n = 58, Kendall rank correlation coefficient, both **P = 0.0002**).

3.5. mRNA levels of shelterin complex subunit TPP1 correlate with TL in tumor tissue

Analysis of the gene expression data obtained by RNA-seq revealed a positive correlation between the *TPP1* mRNA level and the TL measured in the tumor tissue of the patients (n = 52, Kendall rank correlation coefficient, R = 0.21, P = 0.026, see Fig. 4). Further analysis of the RNA-Seq results did not show any correlation between mRNA levels of *hTERT*, encoding the catalytic subunit of telomerase, or the other shelterin subunits (*RAP1*, *TIN2*, *TERF1*, *TERF2*, *POT1*), and TL in the tumor tissue of our studied group of patients (P values not shown).

3.6. Difference in expression profile regarding platinum-based therapy resistance and telomere length

In the end, the whole transcriptome profile analysis was performed beyond shelterin genes, focusing on the expression differences between OvC patients with good and poor response to platinum-based therapy and between OvC patients with telomeres in tumor tissue shorter and longer than the median TL. Primary analysis of the expression profile of OvC patients by principal component

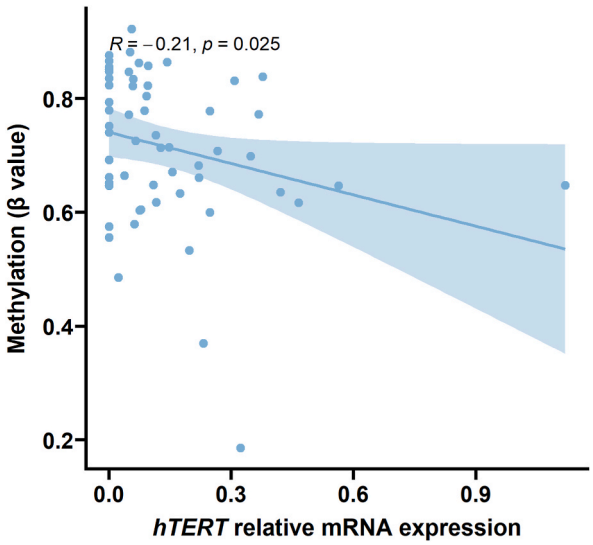

Fig. 3. *hTERT* is expressed in tumors based on the DNA methylation of the promoter sequence. *hTERT* mRNA expression is downregulated due to its promoter TSS1500 methylation (n = 58, R = −0.21, **P = 0.025**).

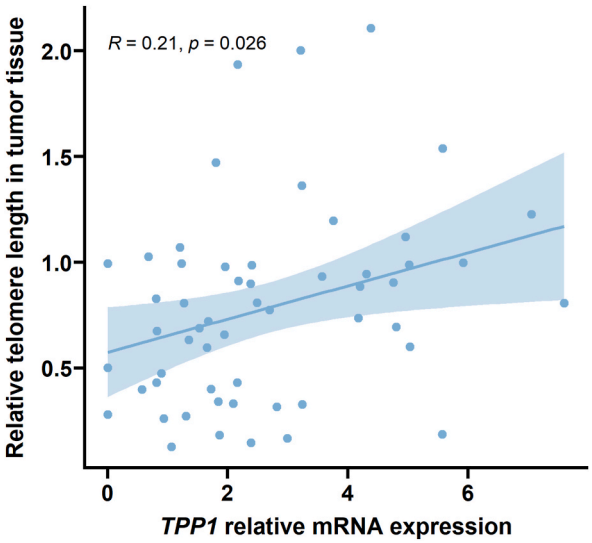

Fig. 4. ***TPP1*** **mRNA expression is associated with TL in tumor tissue.** TL in cancer tissue is positively affected by *TPP1* expression (n = 52, R = 0.21, **P = 0.026**).

analysis (PCA) showed one outlier sample (depicted in Fig. 5A). For further analysis, the sample was removed (see Fig. 5B).

Differential expression (DE) analysis between therapy-sensitive and therapy-resistant OvC patients showed overall 59 significantly differentially expressed genes (q < 0.05, see Fig. 6). Expression downregulation was observed for 42 genes and upregulation for 17 genes. All differentially expressed genes are summarized in Supplementary Table 2.

DE analysis between OvC patients (n = 56) divided into two groups by the median value of TL in tumor tissue showed overall 188 significantly differentially expressed genes (q < 0.05, see Fig. 7). Expression downregulation was observed for 123 genes and upregulation for 65 genes. All differentially expressed genes are in Supplementary Table 3.

In addition, we performed pathway analysis using GO terms (molecular function, biological process, and cellular component) and KEGG pathways for differentially expressed genes. GSEA of GO terms failed to reveal significant (q < 0.05) differences in OvC patients divided by the therapy response, but the first three Top enriched GO terms (**P < 0.001**) were transmembrane receptor protein tyrosine kinase signaling pathway (GO:0007169), response to peptide (GO:1901652), and cellular response to peptide (GO:1901653) for the following genes – nuclear receptor 4A3 (*NR4A3*), adiponectin (*ADIPOQ*), lipoprotein lipase (*LPL*), klotho beta (*KLB*), and polymeric immunoglobulin receptor (*PIGR*), as shown in Fig. 8A and Supplementary Table 4. The KEGG pathway-focused GSEA showed only one significantly enriched pathway – peroxisome proliferator-activated receptor (PPAR) signaling pathway (hsa03320, **q = 0.001**) for cluster determinant 36 (*CD36*), *ADIPOQ*, perilipin 2 (*PLIN2*), and fatty acid binding protein 4 (*FABP4*) genes, as indicated in Supplementary Table 5.

In OvC patients divided by the median TL in tumor tissue, GSEA using GO terms revealed significant (q < 0.05) differences in a total of four significantly enriched terms (**q = 0.026**, see Fig. 8B and Supplementary Table 6) – three cellular components {axonemal microtubule [GO:0005879, genes: cilia and flagella associated protein 45 (*CFAP45*), EF-hand domain containing 2 (*EFHC2*), RIB43A domain with coiled-coils 2 (*RIBC2*)], axoneme [GO:0005930, genes: *CFAP45*, axonemal central pair apparatus protein (*HYDIN*),

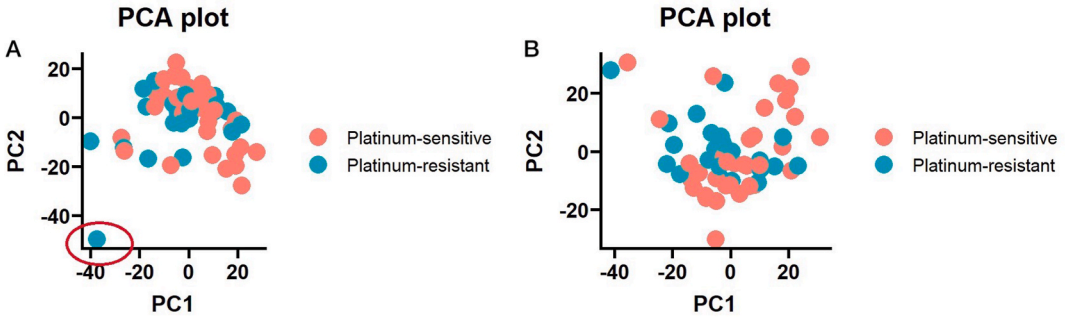

Fig. 5. PCA plot of expression distribution across the ovarian carcinoma set. A) PCA plot of all OvC samples (n = 59) that underwent RNA-Seq, showing one outlier sample in the therapy-resistant group (marked by a red circle). **B)** PCA plot of OvC samples (n = 58) used for further analysis after removing the outlier sample. (For interpretation of the references to color in this figure legend, the reader is referred to the Web version of this article.)

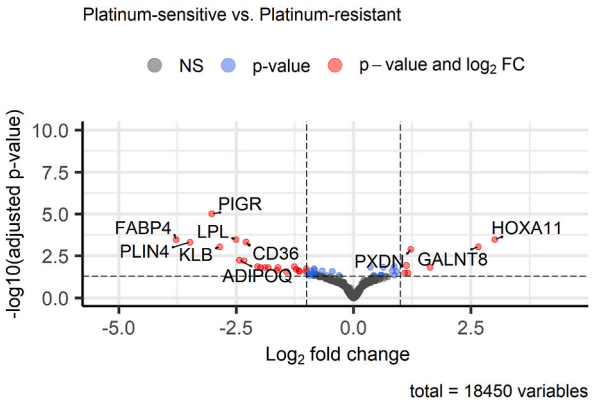

Fig. 6. Expression differences between OvC patients sensitive and resistant to platinum-based therapy. The volcano plot shows the Top 10 differentially expressed genes in the current comparison of 58 OvC patients.

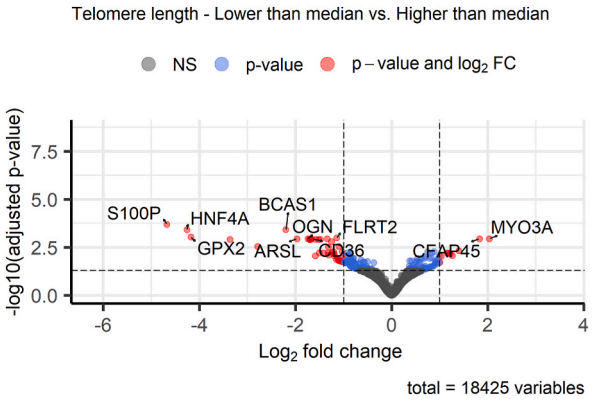

Fig. 7. Expression differences between OvC patients with different lengths of telomeres in tumor tissue. The volcano plot shows the Top 10 differentially expressed genes in the current comparison in the set of 56 OvC patients.

EFHC2, *RIBC2*, cancer susceptibility candidate gene 1 (*CASC1*)] and ciliary plasm (GO:0097014, genes: *CFAP45*, *HYDIN*, *EFHC2*, *RIBC2*, *CASC1*)} and one biological process [DNA metabolic process, GO:0006259, genes: retinoblastoma-binding protein 8 (*RBBP8*), nuclear autoantigenic sperm protein (*NASP*), B-cell CLL/lymphoma 7 A (*BCL7A*), YEATS domain containing 4 (*YEATS4*), structural maintenance of chromosomes 1 A (*SMC1A*), structure specific recognition protein 1 (*SSRP1*), heterogenous nuclear ribonucleoprotein A/B (*HNRNPAB*), lysine demethylase 2 A (*KDM2A*), dyskerin pseudouridine synthase 1 (*DKC1*), DNA polymerase epsilon 3 (*POLE3*), DNA helicase and adenosine triphosphatase (*UPF1*), fragile X messenger ribonucleoprotein 1 (*FMR1*)]. GSEA did not identify significant ($q < 0.05$) KEGG pathway differences between the two groups of OvC patients divided by the TL in tumor tissue. However, the first three Top enriched pathways (listed in Supplementary Table 5) were: adenosine monophosphate-activated protein kinase (AMPK) signaling pathway [hsa04152, genes: *CD36*, hepatocyte nuclear factor 4 alpha (*HNF4A*), **P = 0.007**], leukocyte transendothelial migration [hsa04670, genes: claudin 11 (*CLDN11*), junction adhesion molecule 3 (*JAM3*), claudin 18 (*CLDN18*), **P = 0.02**], and cell adhesion molecules (hsa04514, genes: *CLDN11, JAM3, CLDN18*, **P = 0.023**).

4. Discussion

Earlier studies suggested that OvC, a heterogeneous group of diseases with multifactorial etiopathogenesis, may exhibit telomere dysfunction [10,11]. In addition, ovarian carcinomas appear to be strictly telomerase-dependent. More than 95 % of ovarian tumors are hallmarked with substantial *hTERT* expression, a limiting factor for telomerase catalytical activity [10]. Harboring of *hTERT* promoter mutation was reported in 16 % of clear cell OvC [12,13] and 50 % of granulosa cell tumors [14]. Our knowledge of shelterin alteration in OvC is considerably modest. Yet, *POT1* knockdown in OvC-derived SK-OV3 cells reduces the expression of *c-Myc*, triggering temporary inhibition of proliferation but ultimately resulting in enhanced cell division, tumorigenicity, and histone deacetylase inhibitor response [15].

In this, we investigated whether TL in tumor tissue and PBL from patients diagnosed with OvC may relate to their therapy response and prognosis. Here we document, for the first time, that the response of the OvC patients to treatment is ameliorated in the patients with shorter TL in PBL, and patients' survival is significantly longer in patients with shorter TL in tumor tissue. We also recorded

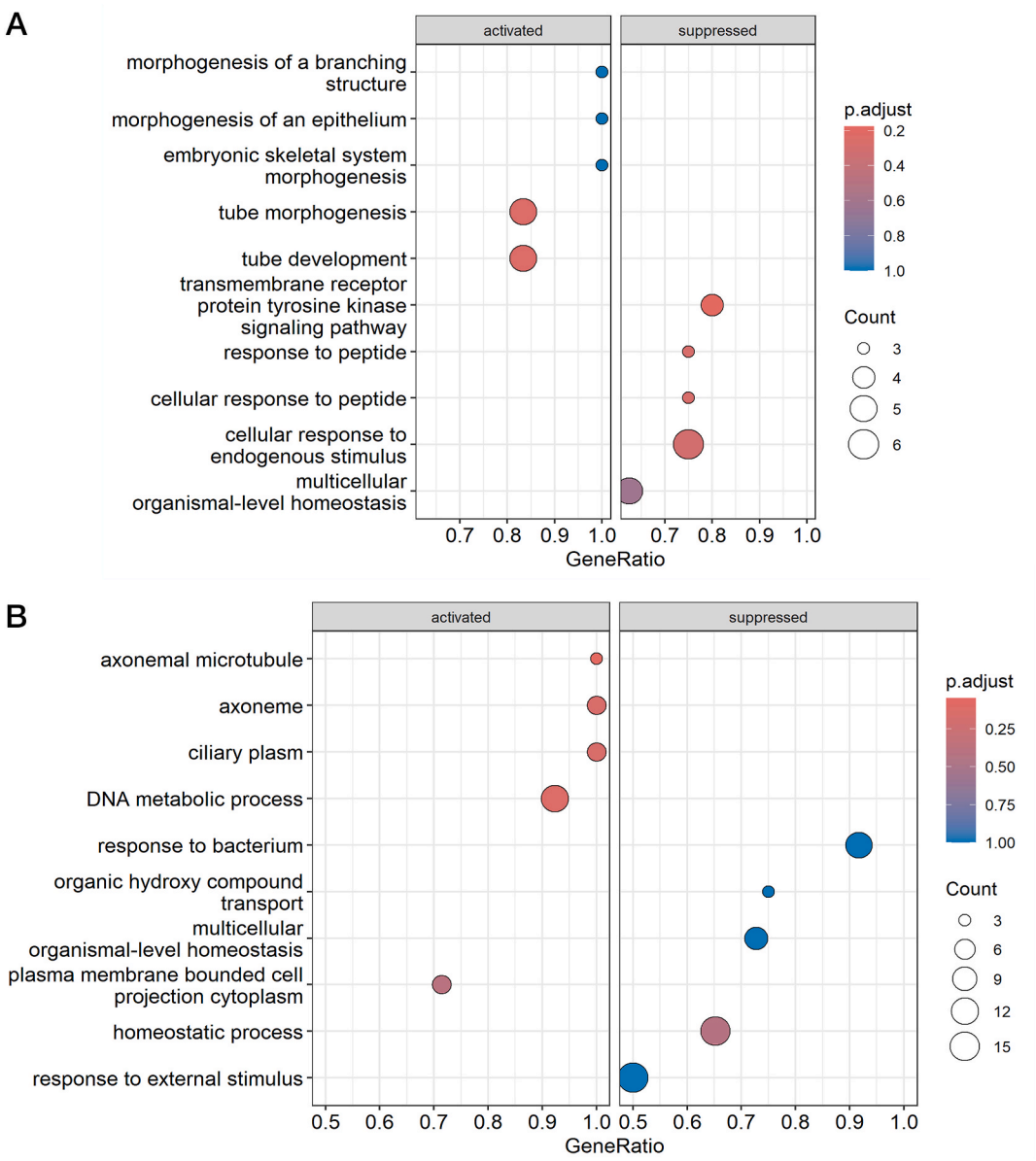

Fig. 8. Results of GSEA for GO terms. A) The dotplot represents the Top 10 enriched GO terms for differentially expressed genes from the therapy response analysis. **B)** The dotplot shows the Top 10 enriched GO terms for differentially expressed genes from the tumor TL analysis.

intriguing associations between the mRNA expression and DNA methylation of shelterin subunits, telomerase, and TL.

Consistent with the literature, this study found that prolonged TL in tumors may implicate worse OS of patients diagnosed with OvC. Previously, worse OS in patients with long tumor telomeres (index >1, defined as the ratio of relative mean TL of tumor cells/stromal cells) was confirmed exclusively for clear cell histologic type but not for a whole studied set [42]. On the contrary, no relationship between OvC-specific mortality and TL likely exists in PBL, as previously shown by Kotsopoulos et al. [43].

Our data show that longer PBL TL might be bound up with the onset of therapy resistance. Those patients evaluated as resistant had progressive tumors, low tolerance to neo-/adjuvant chemotherapy, or experienced a rapid relapse. However, conflicting results were described by Falandry et al. [44]. In the study, the OvC patients with longer TL in lymphocytes (>5.77 kb) showed better treatment tolerance (2.7 odds ratio) and a higher probability of therapy completion than those with shorter TL (80 % rate vs. 59 % rate) [44]. In addition, longer lymphocyte TL was associated with less frequent unplanned hospital admissions and lower grade 3–4 non-hematological toxicity (2.14 and 2.04 odds ratio, respectively) [44]. Signs that chemotherapy may impact telomere maintenance machinery, and thus presumably TL, have been proven *in vitro*. In epithelial OvC cell line HO8910, telomerase activity and *hTERT* expression alternations have been shown to reflect the effect of cisplatin [45].

It should be emphasized that elevated production of TPP1, which, in complex with POT1 and telomeric DNA, recruits telomerase

and stimulates its processivity [46], is connected to telomere elongation. We observed that tumoral *TPP1* mRNA expression positively correlates with TL, just as Yang et al. had reported the relationship between TPP1 protein levels in colorectal cancer cell lines [47]. In addition, the study authors stated that TPP1 protein overexpression and longer telomeres are linked to radioresistance. However, we did not find any association between shelterin-subunit mRNA level and therapy response, although the size of the studied group and the OvC heterogeneity might have obscured the association. Furthermore, we observed that *hTERT* promoter methylation down-regulates *hTERT* mRNA expression and leads to shorter telomeres. Previously, Widschwendter et al. related the *hTERT* expression in OvC tissue only to the methylation of the whole gene, where the association was not found [48]. Besides *hTERT* methylation patterns, we associated several methylation statuses of shelterin (*TERF1*, *TERF2*, *POT1*, *RAP1*) with OvC tissue TL. Our study suggests the importance of telomere biology in the prognosis and treatment prediction of OvC patients.

Analysis of whole transcriptome profiles revealed other important candidates for further detailed studies involving telomerase activity in ovarian tumors. Our data show that differentially expressed genes from analysis focused on OvC patients with different lengths of telomeres in tumor tissue (divided by median value) were enriched in pathways associated with cell adhesion, AMPK signaling pathway, and leukocyte *trans*-endothelial migration. In our case, the most prominent genes were *JAM3, CLDN11,* and *CLDN18*. For the genes, we found no reported connection with ovarian carcinoma therapy resistance or telomerase activity. However, there is evidence of an indirect role of hTERT in cell adhesion, migration (e.g., in sarcoma cancer cell line U2OS) or in cancer stemness and metastasis [49,50]. In breast cancer, *in vitro* and *in vivo* models enhanced sensitivity to doxorubicin and alteration in adhesion pathways after hTERT downregulation were observed [51]. These findings show another possible indirect role of telomerase biology in the progression of OvC.

Functional annotation of differentially expressed genes based on therapy response showed alterations in the PPAR signaling pathway (KEGG database) and tyrosine kinase signaling pathway with peptide response (GO terms). The genes enriched in these pathways were *PLIN2, ADIPOQ1, FABP4, NR4A3, KLB, LPL, PIGR* and *CD36*. ADIPOQ1 gene is a joint member of all the above mentioned pathways. The PPAR signaling pathway is often altered in cancer tissue, and members of this pathway (*PLIN2* and *ADIPOQ1*) are key parts of adipocyte differentiation. The role of adipocytes in OvC progression is currently being studied, and results are showing their importance in cancer progressiveness [52,53]. In addition, another candidate *FABP4*, mainly expressed in adipocytes, is connected with OvC progression, resistance to platinum derivatives, and, thus, poor prognosis [54,55]. CD36 molecule, another member of fatty acid metabolism associated with therapy response in our study, is also connected with OvC progression, the metastasis process, and platinum derivatives resistance [56–58]. Moreover, CD36 is considered to be a potential therapeutic target. Novel therapeutics such as photoactivable Pt(IV) metallodrugs targeting CD36-positive OvC cells have already been prepared and tested, and showed their efficiency in eliminating drug-resistant OvC cells [59]. These results support the importance of adipocytes and lipid metabolism in OvC and in cancer in general.

The study offers numerous advantages alongside certain constraints. Our current study's merit lies in comparing TL between blood and tumor tissue DNA in a carefully chosen and similar clinical cohort characterized by advanced stage, grade, well-documented PFI, and shared ethnicity (Slavic Caucasian). This focus is particularly beneficial given the scarcity of studies addressing this aspect. Furthermore, TL examination alongside the gene expression and methylation profile of the shelterin complex within the same patient cohort adds another layer of value to our investigation. However, our study's limitation is its relatively modest sample size, although this is mitigated by the thorough selection and characterization of the patient group.

5. Conclusions

We compared OvC tissue TL with mRNA expression and DNA methylation data of telomerase and shelterin and analyzed TL in PBL. This study found that prolonged TL in tumors may implicate worse OS of patients diagnosed with OvC. Our data showed that longer PBL TL might be bound up with the onset of therapy resistance. DNA methylation analysis of shelterin and telomerase genes identified *TERF1*, *TERF2*, *TPP1*, *RAP1*, and *hTERT* CpG sites at which methylation levels are associated with TL in tumors. We also found that TL in tumors positively relates to the gene expression of *TPP1* and that *hTERT* mRNA expression is inversely proportional to its promoter methylation level. The study also showed the possible involvement of telomerase in the migratory potential of cancer cells and the role of adipocytes/lipid metabolism in OvC progression.

Funding

The work was supported by the Czech Science Foundation [19-10543 S (**PV**), 21-27902 S (**LV**)]; the Czech Health Research Council grant [NU21-03-00145 (**LV, RV**)]; and the Cooperatio programs [207035, "Maternal and Childhood Care", 3rd Faculty of Medicine, Charles University (**LR**), 207043, "Surgical Disciplines", Faculty of Medicine in Pilsen, Charles University (**KT**,**LV**,**RV**,**PV**)]. We also acknowledge the project NPO [LX22NPO5102 (**LV**)].

Ethics statement and consent to participate

This study was reviewed and approved by the Institutional Review Boards of the National Institute of Public Health in Prague (approval number: IGA NS9803-4, dated January 30, 2008), the University Hospital Kralovske Vinohrady (approval number: EK-VP/25/0/2018, dated June 6, 2018), the University Hospital in Pilsen (approval number: 16–29013 A, dated June 7, 2018), and the University Hospital in Motol (approval number: EK-890/15, dated June 24, 2015). All participants/patients (or their proxies/legal guardians) provided written informed consent to participate in the study.

Data availability statement

RNA-Seq dataset generated and analyzed during the current study is available in the NCBI BioProject repository, https://www.ncbi.nlm.nih.gov/, BioProject ID: PRJNA866991. Methylation and TL datasets generated during the current study are available from the corresponding author on reasonable request.

CRediT authorship contribution statement

Kristyna Tomasova: Writing – original draft, Investigation. **Karolina Seborova:** Writing – review & editing, Investigation, Formal analysis, Data curation. **Michal Kroupa:** Writing – original draft, Investigation. **Josef Horak:** Visualization, Formal analysis. **Miriam Kavec:** Investigation. **Ludmila Vodickova:** Project administration, Funding acquisition. **Lukas Rob:** Resources, Funding acquisition. **Martin Hruda:** Resources. **Marcela Mrhalova:** Resources. **Alena Bartakova:** Resources. **Jiri Bouda:** Resources. **Thomas Fleischer:** Investigation, Formal analysis. **Vessela N. Kristensen:** Supervision. **Pavel Vodicka:** Writing – review & editing, Supervision, Project administration, Funding acquisition, Conceptualization. **Radka Vaclavikova:** Writing – review & editing, Supervision, Project administration, Funding acquisition, Conceptualization.

Declaration of competing interest

The authors declare that they have no known competing financial interests or personal relationships that could have appeared to influence the work reported in this paper.

Acknowledgements

We would like to thank the Genomics Core Facility, Oslo University Hospital (http://oslo.genomics.no/), for performing methylation array analysis.

Appendix A. Supplementary data

Supplementary data to this article can be found online at https://doi.org/10.1016/j.heliyon.2024.e33525.

References

[1] N. Srinivas, S. Rachakonda, R. Kumar, Telomeres and telomere length: a general overview, Cancers 12 (2020) 558, https://doi.org/10.3390/cancers12030558.
[2] K. Tomasova, M. Kroupa, A. Forsti, P. Vodicka, L. Vodickova, Telomere maintenance in interplay with DNA repair in pathogenesis and treatment of colorectal cancer, Mutagenesis (2020) 35261–35271, https://doi.org/10.1093/mutage/geaa005.
[3] T. de Lange, Shelterin-mediated telomere protection, Annu. Rev. Genet. 52 (2018) 223–247, https://doi.org/10.1146/annurev-genet-032918-021921.
[4] C. Hu, R. Rai, C. Huang, et al., Structural and functional analyses of the mammalian TIN2-TPP1-TRF2 telomeric complex, Cell Res. 27 (2017) 1485–1502, https://doi.org/10.1038/cr.2017.144.
[5] T. Kibe, M. Zimmermann, T. de Lange, TPP1 blocks an ATR-mediated resection mechanism at telomeres, Mol. Cell 61 (2016) 236–246, https://doi.org/10.1016/j.molcel.2015.12.016.
[6] J. Maciejowski, T. de Lange, Telomeres in cancer: tumour suppression and genome instability, Nat. Rev. Mol. Cell Biol. 18 (2017) 175–186, https://doi.org/10.1038/nrm.2016.171.
[7] A.J. Cesare, R.R. Reddel, Alternative lengthening of telomeres: models, mechanisms and implications, Nat. Rev. Genet. 11 (2010) 319–330, https://doi.org/10.1038/nrg2763.
[8] W.C. Hahn, M. Meyerson, Telomerase activation, cellular immortalization and cancer, Ann. Med. 33 (2001) 123–129, https://doi.org/10.3109/07853890109002067.
[9] C.B. Harley, Telomerase and cancer therapeutics, Nat. Rev. Cancer 8 (2008) 167–179, https://doi.org/10.1038/nrc2275.
[10] N. Huda, Y. Xu, A.M. Bates, et al., Onset of telomere dysfunction and fusions in human ovarian carcinoma, Cells 8 (2019) 414, https://doi.org/10.3390/cells8050414.
[11] S.E. Bojesen, K.A. Pooley, S.E. Johnatty, et al., Multiple independent variants at the TERT locus are associated with telomere length and risks of breast and ovarian cancer, Nat. Genet. 45 (2013) 371–384, https://doi.org/10.1038/ng.2566.
[12] H.-N. Huang, Y.-C. Chiang, W.-F. Cheng, et al., Molecular alterations in endometrial and ovarian clear cell carcinomas: clinical impacts of telomerase reverse transcriptase promoter mutation, Mod. Pathol. 28 (2015) 303–311, https://doi.org/10.1038/modpathol.2014.93.
[13] R.-C. Wu, A. Ayhan, D. Maeda, et al., Frequent somatic mutations of the telomerase reverse transcriptase promoter in ovarian clear cell carcinoma but not in other major types of gynaecological malignancy, J. Pathol. 232 (2014) 473–481, https://doi.org/10.1002/path.4315.
[14] J.A. Pilsworth, D.R. Cochrane, Z. Xia, et al., TERT promoter mutation in adult granulosa cell tumor of the ovary, Mod. Pathol. 31 (2018) 1107–1115, https://doi.org/10.1038/s41379-018-0007-9.
[15] H. Zhou, A. Mondal, A. Dakic, et al., Time-dependent effects of POT1 knockdown on proliferation, tumorigenicity, and HDACi response of SK-OV3 ovarian cancer cells, BioMed Res. Int. 2018 (2018) 7184253, https://doi.org/10.1155/2018/7184253.
[16] R.A. Greenberg, R.C. O'Hagan, H. Deng, et al., Telomerase reverse transcriptase gene is a direct target of c-Myc but is not functionally equivalent in cellular transformation, Oncogene 18 (1999) 1219–1226, https://doi.org/10.1038/sj.onc.1202669.
[17] S. Karami, Y. Han, M. Pande, et al., Telomere structure and maintenance gene variants and risk of five cancer types, Int. J. Cancer 139 (2016) 2655–2670, https://doi.org/10.1002/ijc.30288.
[18] M. Friedlander, E. Trimble, A. Tinker, et al., Clinical trials in recurrent ovarian cancer, Int. J. Gynecol. Cancer 21 (2011) 771–775, https://doi.org/10.1097/IGC.0b013e31821bb8aa.
[19] M. Kroupa, S.K. Rachakonda, V. Liska, et al., Relationship of telomere length in colorectal cancer patients with cancer phenotype and patient prognosis, Br. J. Cancer 121 (2019) 344–350, https://doi.org/10.1038/s41416-019-0525-3.

[20] M. Kroupa, S. Rachakonda, V. Vymetalkova, et al., Telomere length in peripheral blood lymphocytes related to genetic variation in telomerase, prognosis and clinicopathological features in breast cancer patients, Mutagenesis 35 (2020) 491–497, https://doi.org/10.1093/mutage/geaa030.
[21] S. Guenin, M. Mauriat, J. Pelloux, et al., Normalization of qRT-PCR data: the necessity of adopting a systematic, experimental conditions-specific, validation of references, J. Exp. Bot. 60 (2009) 487–493, https://doi.org/10.1093/jxb/ern305.
[22] S. Andrews, FastQC: a quality control tool for high throughput sequence data (2010). Seen 9. 6. 2024. Available online at: http://www.bioinformatics.babraham.ac.uk/projects/fastqc.
[23] P. Ewels, M. Magnusson, S. Lundin, et al., MultiQC: summarize analysis results for multiple tools and samples in a single report, Bioinforma Oxf Engl 32 (2016) 3047–3048, https://doi.org/10.1093/bioinformatics/btw354.
[24] S. Chen, Y. Zhou, Y. Chen, et al., fastp: an ultra-fast all-in-one FASTQ preprocessor, Bioinformatics 34 (2018) 884–890, https://doi.org/10.1093/bioinformatics/bty560.
[25] N.L. Bray, H. Pimentel, P. Melsted, et al., Near-optimal probabilistic RNA-seq quantification, Nat. Biotechnol. 34 (2016) 525–527, https://doi.org/10.1038/nbt0816-888d.
[26] M.I. Love, W. Huber, S. Anders, Moderated estimation of fold change and dispersion for RNA-seq data with DESeq2, Genome Biol. 15 (2014) 550, https://doi.org/10.1186/s13059-014-0550-8.
[27] M. Stephens, False discovery rates: a new deal, Biostatistics 18 (2016) 275–294, https://doi.org/10.1093/biostatistics/kxw041.
[28] T. Wu, E. Hu, S. Xu, et al., clusterProfiler 4.0: a universal enrichment tool for interpreting omics data, Innovation 2 (2021) 100141, https://doi.org/10.1016/j.xinn.2021.100141.
[29] G. Yu, L.-G. Wang, G.-R. Yan, et al., DOSE: an R/Bioconductor package for disease ontology semantic and enrichment analysis, Bioinformatics 31 (2015) 608–609, https://doi.org/10.1093/bioinformatics/btu684.
[30] M. Ashburner, C.A. Ball, J.A. Blake, et al., Gene Ontology: tool for the unification of biology, Nat. Genet. 25 (2000) 25–29, https://doi.org/10.1038/75556.
[31] The Gene Ontology Consortium, S.A. Aleksander, J. Balhoff, S. Carbon, et al., The gene ontology knowledgebase in 2023, Genetics 224 (2023) 31, https://doi.org/10.1093/genetics/iyad031.
[32] M. Kanehisa, M. Furumichi, Y. Sato, et al., KEGG for taxonomy-based analysis of pathways and genomes, Nucleic Acids Res. 51 (2023) 587–592, https://doi.org/10.1093/nar/gkac963.
[33] R Core Team, European Environment Agency (2020). Seen 9. 6. 2024. Available online at: https://www.eea.europa.eu/data-and-maps/indicators/oxygen-consuming-substances-in-rivers/r-development-core-team-2006.
[34] N. Touleimat, J. Tost, Complete pipeline for Infinium® Human Methylation 450K BeadChip data processing using subset quantile normalization for accurate DNA methylation estimation, Epigenomics 4 (2012) 325–341, https://doi.org/10.2217/epi.12.21.
[35] T. Fleischer, A. Frigessi, K.C. Johnson, et al., Genome-wide DNA methylation profiles in progression to in situand invasive carcinoma of the breast with impact on gene transcription and prognosis, Genome Biol. 15 (2014) 435, https://doi.org/10.1186/PREACCEPT-2333349012841587.
[36] J.-P. Fortin, T.J. Triche, K.D. Hansen, Preprocessing, normalization and integration of the Illumina HumanMethylationEPIC array with minfi, Bioinformatics 33 (2016) 558–560, https://doi.org/10.1093/bioinformatics/btw691.
[37] J. Maksimovic, L. Gordon, A. Oshlack, SWAN: subset-quantile within array normalization for Illumina Infinium HumanMethylation450 BeadChips, Genome Biol. 13 (2012) 44, https://doi.org/10.1186/gb-2012-13-6-r44.
[38] P. Du, X. Zhang, C.-C. Huang, et al., Comparison of Beta-value and M-value methods for quantifying methylation levels by microarray analysis, BMC Bioinf. 11 (2010) 587, https://doi.org/10.1186/1471-2105-11-587.
[39] R. Pidsley, E. Zotenko, T.J. Peters, et al., Critical evaluation of the Illumina MethylationEPIC BeadChip microarray for whole-genome DNA methylation profiling, Genome Biol. 17 (2016) 208, https://doi.org/10.1186/s13059-016-1066-1.
[40] K. Seborova, V. Hlavac, P. Holy, et al., Complex molecular profile of DNA repair genes in epithelial ovarian carcinoma patients with different sensitivity to platinum-based therapy, Front. Oncol. 12 (2022) 1016958, https://doi.org/10.3389/fonc.2022.1016958.
[41] M. Bibikova, J. Le, B. Barnes, et al., Genome-wide DNA methylation profiling using Infinium® assay, Epigenomics 1 (2009) 177–200, https://doi.org/10.2217/epi.09.14.
[42] E. Kuhn, A.K. Meeker, K. Visvanathan, et al., Telomere length in different histologic types of ovarian carcinoma with emphasis on clear cell carcinoma, Mod. Pathol. 24 (2011) 1139–1145, https://doi.org/10.1038/modpathol.2011.67.
[43] J. Kotsopoulos, J. Prescott, I. De Vivo, et al., Telomere length and mortality following a diagnosis of ovarian cancer, Cancer Epidemiol. Biomark. Prev. 23 (2014) 2603–2606, https://doi.org/10.1158/1055-9965.EPI-14-0885.
[44] C. Falandry, B. Horard, A. Bruyas, et al., Telomere length is a prognostic biomarker in elderly advanced ovarian cancer patients: a multicenter GINECO study, Aging 7 (2015) 1066–1076, https://doi.org/10.18632/aging.100840.
[45] P.-M. Sun, L.-H. Wei, M.-Y. Luo, et al., The telomerase activity and expression of hTERT gene can serve as indicators in the anti-cancer treatment of human ovarian cancer, Eur. J. Obstet. Gynecol. Reprod. Biol. 130 (2007) 249–257, https://doi.org/10.1016/j.ejogrb.2006.01.028.
[46] A.J. Zaug, E.R. Podell, J. Nandakumar, T.R. Cech, Functional interaction between telomere protein TPP1 and telomerase, Genes Dev. 24 (2010) 613–622, https://doi.org/10.1101/gad.1881810.
[47] L. Yang, W. Wang, L. Hu, et al., Telomere-binding protein TPP1 modulates telomere homeostasis and confers radioresistance to human colorectal cancer cells, PLoS One 8 (2013) 81034, https://doi.org/10.1371/journal.pone.0081034.
[48] A. Widschwendter, H. Muller, M. Hubalek, et al., Methylation status and expression of human telomerase reverse transcriptase in ovarian and cervical cancer, Gynecol. Oncol. 93 (2004) 407–416, https://doi.org/10.1016/j.ygyno.2004.01.036.
[49] H. Liu, Q. Liu, Y. Ge, et al., hTERT promotes cell adhesion and migration independent of telomerase activity, Sci. Rep. 6 (2016) 22886, https://doi.org/10.1038/srep22886.
[50] R. Hannen, J.W. Bartsch, Essential roles of telomerase reverse transcriptase hTERT in cancer stemness and metastasis, FEBS Lett. 592 (2018) 2023–2031, https://doi.org/10.1002/1873-3468.13084.
[51] A. Romaniuk-Drapała, E. Toton, N. Konieczna, et al., hTERT downregulation attenuates resistance to DOX, impairs FAK-mediated adhesion, and leads to autophagy induction in breast cancer cells, Cells 10 (2021) 867, https://doi.org/10.3390/cells10040867.
[52] T. Chi, M. Wang, X. Wang, et al., PPAR-γ modulators as current and potential cancer treatments, Front. Oncol. 11 (2021) 737776, https://doi.org/10.3389/fonc.2021.737776.
[53] L. Dai, K. Song, W. Di, Adipocytes: active facilitators in epithelial ovarian cancer progression? J. Ovarian Res. 13 (2020) 115, https://doi.org/10.1186/s13048-020-00718-4.
[54] A. Mukherjee, C.-Y. Chiang, H.A. Daifotis, et al., Adipocyte-induced FABP4 expression in ovarian cancer cells promotes metastasis and mediates carboplatin resistance, Cancer Res. 80 (2020) 1748–1761, https://doi.org/10.1158/0008-5472.CAN-19-1999.
[55] K.M. Gharpure, S. Pradeep, M. Sans, et al., FABP4 as a key determinant of metastatic potential of ovarian cancer, Nat. Commun. 9 (2018) 2923, https://doi.org/10.1038/s41467-018-04987-y.
[56] M. Jiang, R. Karsenberg, F. Bianchi, et al., CD36 as a double-edged sword in cancer, Immunol. Lett. 265 (2024) 7–15, https://doi.org/10.1016/j.imlet.2023.12.002.
[57] A. Ladanyi, A. Mukherjee, H.A. Kenny, et al., Adipocyte-induced CD36 expression drives ovarian cancer progression and metastasis, Oncogene 37 (2018) 2285–2301, https://doi.org/10.1038/s41388-017-0093-z.
[58] S. Zhou, R. Wang, H. Xiao, Adipocytes induce the resistance of ovarian cancer to carboplatin through ANGPTL4, Oncol. Rep. 44 (2020) 927–938, https://doi.org/10.3892/or.2020.7647.
[59] A.M.D.S. Jayawardhana, S. Bhandari, A.W. Kaspi-Kaneti, et al., Visible light-activatable platinum(IV) prodrugs harnessing CD36 for ovarian cancer therapy, Dalton Trans. 52 (2023) 10942–10950, https://doi.org/10.1039/d3dt01292a.